

ACCRETION DISKS IN ACTIVE GALACTIC NUCLEI: GAS SUPPLY DRIVEN BY STAR FORMATION

JIAN-MIN WANG, CHANG-SHUO YAN, HAN-QIN GAO, CHEN HU, YAN-RONG LI AND SHU ZHANG
 Key Laboratory for Particle Astrophysics, Institute of High Energy Physics, Chinese Academy of Sciences,
 19B Yuquan Road, Beijing 100049, China

Received 2010 April 14; accepted 2010 July 14

ABSTRACT

Self-gravitating accretion disks collapse to star-forming(SF) regions extending to the inner edge of the dusty torus in active galactic nuclei (AGNs). A full set of equations including feedback of star formation is given to describe the dynamics of the regions. We explore the role of supernovae explosion (SNexp), acting to excite turbulent viscosity, in the transportation of angular momentum in the regions within 1pc scale. We find that accretion disks with typical rates in AGNs can be driven by SNexp in the regions and metals are produced spontaneously. The present model predicts a metallicity–luminosity relationship consistent with that observed in AGNs. As relics of SF regions, a ring (or belt) consisting of old stars remains for every episode of supermassive black hole activity. We suggest that multiple stellar rings with random directions interact and form a nuclear star cluster after episodes driven by star formation.

Subject headings: accretion disks - quasars: general - stars: formation

1. INTRODUCTION

Accretion onto supermassive black holes (SMBHs) is the energy house of active galactic nuclei (AGNs). Applying models of accretion disks to fit the observed big blue bumps in the continuum of AGNs and quasars, one finds that SMBHs accrete typically with sub-Eddington rates (Laor & Netzer 1989; Sun & Malkan 1989; Brunner et al. 1997; Lü 2008). Observational examination of the Soltan argument for the cosmological growth of SMBHs prefers that they grow episodically through baryon accretion (Yu & Tremaine 2002; Wang et al. 2009a), in agreement with the paradigm of coevolution with their host galaxies. However, what is governing accretion rates of active SMBHs?

We have several relevant clues to understanding the formation of the accretion flows approaching SMBHs at ~ 1 pc scale. First, the well-known metallicity and luminosity relationship in AGNs and quasars (see a review of Hamann & Ferland 1999) strongly implies that the flows may undergo *fast* metal productions through stellar evolution in active episodes in light of the absence of cosmic evolution of metallicity (Dietrich et al. 2003; Shemmer et al. 2004). This gets supports from evidence that there is intensive star formation with the top-heavy initial mass function (IMF) within ~ 0.1 pc in the Galactic center (Paumard et al. 2006; Nayakshin & Sunyaev 2005) confirmed by numerical simulations (Nayakshin et al. 2007; Bonnell & Rice 2008; Hobbs & Nayakshin 2009). We may naturally postulate that accretion onto SMBHs is the consequence of metal production. Second, it has long been known that accretion disks in quasars are massive and self-gravitating in outer regions (Paczynski 1978; Kolykhalov & Sunyaev 1980; Shlosman & Begelman 1987; Collin & Zahn 1999). Obviously, the self-gravity is driving intensive star formation ongoing there (Goodman 2003), and a star-forming (SF) disk (or regions) appears. It seems that there is no way to avoid the production of metals and trigger accretion flows in the SF disk, yielding the metallicity–luminosity relationship. We argue that SNexp plays a leading role in the establishment of the relationship in light of SNexp-excited turbulent viscosity as shown in the ~ 1 kpc regions by numerical simulations (Wada & Norman 2002; Hobbs et al. 2010) or physical moti-

vation (Wang et al. 2009b; see also Kumar & Johnson 2010) and $\sim 10^4$ Sloan type 2 AGNs (Chen et al. 2009). Furthermore, we are inspired by the recent evidence for that the "visible" inflows displayed by the $H\beta$ line are likely developed from the inner edge of the dusty torus in ~ 5000 Sloan quasars (Hu et al. 2008a,2008b). All clues merge into a question: are accretion inflows driven by star formation in the massive self-gravitating disk?

In this Letter, we show the feasibility that an SF disk is able to drive a Shakura–Sunyaev disk (hereafter SS disk) in AGNs through SNexp-excited turbulent viscosity. We find that such a scenario agrees with observations of metallicity and results in the formation of a nuclear star cluster potentially.

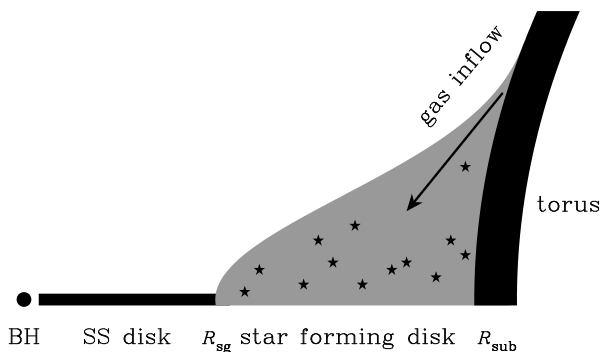


FIG. 1.— Schematic illustration of the present model. The SF disk starts from the inner edge of the dusty torus (R_{sub}) and switches on the SS disk at the self-gravity radius (R_{sg}).

2. BASIC EQUATIONS

Figure 1 shows an illustration of the present model. The outer boundary of the SF disk (R_{out}) is chosen at the inner edge of the torus as suggested by Hu et al. (2008a,2008b), where dust particles are sublimated at $R_{\text{sub}} = 1.3L_{\text{UV},46}^{1/2}$ pc, where $L_{\text{UV},46} = L_{\text{UV}}/10^{46}$ erg s^{-1} (Barvainis 1987). The option of $R_{\text{out}} = R_{\text{sub}}$ is motivated by a fact that emission from $R \geq R_{\text{sub}}$ is invisible in optics. Collisions of molecular clouds transfer angular momentum outward and supply gas to the SF disk with a rate of $\dot{M}_{\text{out}} = 1 \sim 20M_{\odot}\text{yr}^{-1}$ at R_{sub} from the

torus (Krolik & Begelman 1988) with a typical mass range of $10^5 \sim 10^7 M_\odot$ (Mor et al. 2009). This typical mass is just at the level required by a single episode of SMBH activity.

2.1. SNexp-driven gaseous disk

With the inclusion of the mass dropout from star formation and the injection of gas recycled from SNexp, the mass conservation equation for the SF disk reads¹

$$\frac{\partial \Sigma_{\text{gas}}}{\partial t} = \frac{1}{2\pi R} \frac{\partial}{\partial R} \left\{ \left[\frac{d(R^2 \Omega)}{dR} \right]^{-1} \frac{\partial \mathcal{G}}{\partial R} \right\} - \dot{\Sigma}_* + \dot{\Sigma}_{\text{SN}}, \quad (1)$$

where Σ_{gas} is the surface density, $\mathcal{G} = -2\pi R^3 \nu \Sigma_{\text{gas}} (d\Omega/dR)$ is the viscosity torque, ν is the kinematic viscosity, Ω is the angular velocity, $\dot{\Sigma}_*$ is the surface density of star formation rates, and $\dot{\Sigma}_{\text{SN}}$ is the injection rate of gas recycled from SNexp. We use the relation $\dot{\Sigma}_{\text{SN}} = f_c \dot{\Sigma}_*$, where f_c is the fraction of the SNexp-ejected mass to the total formed stars. For an episodic activity of AGN with Δt_G (e.g., Wang et al. 2006), the minimum mass of the stars producing an SNexp should be $M_c/M_\odot \geq 7.0 \Delta t_{0.1}^{-0.4}$, where the lifetime of hydrogen main-sequence stars is $t_{\text{MS}} = 13 (M_*/M_\odot)^{-2.5}$ Gyr and $\Delta t_{0.1} = \Delta t_G/0.1$ Gyr. Assuming an IMF as $N(M_*)dM_* = N_0 M_*^{-\beta} dM_*$, we have $f_c = \int_{M_c}^{100M_\odot} M_* N(M_*) dM_*/M_{\text{tot}}$, where $M_{\text{tot}} = \int_{M_{\text{min}}}^{100M_\odot} M_* N(M_*) dM_*$ is the total mass of the formed stars. It follows $f_c \sim 0.38$ for the Salpeter IMF $\beta = 2.35$, $M_{\text{min}} = 1.0M_\odot$, and $M_c = 7M_\odot$, meaning that a significant mass fraction of the formed stars will be injected into the SF disk from SNexp (here we neglect the remnant compact stars after SNexp). The scale influenced by an SNexp is of the order of $D_{\text{SN}} \sim (E_{\text{SN}}/m_p n c_s^2)^{1/3} \sim 0.1 E_{51}^{1/3} (n_{11} T_3)^{-1/3}$ pc, where $E_{51} = E_{\text{SN}}/10^{51}$ erg is the kinetic energy of SNexp, $n_{11} = n_{\text{gas}}/10^{11} \text{cm}^{-3}$ is the number density of the medium in the SF disk, $c_s \approx 3.0 \times 10^5 T_3^{1/2} \text{cm s}^{-1}$ is the isothermal sound speed, and $T_3 = T/10^3 \text{K}$ is the temperature. We find from this simple estimation that the length of the SNexp influence is comparable with the height of the SF disk (~ 0.1 pc) and the SNexp-excited turbulence velocity $V_{\text{tur}} \gg c_s$, and hence SNexp plays a key role in the transportation of angular momentum.

In this Letter, we focus on the stationary case, namely, $\partial \Sigma_{\text{gas}}/\partial t = 0$. Introducing the parameter $X = R^2 \Omega$, Equation (1) is rewritten as

$$\frac{1}{2\pi R} \frac{dX}{dR} \frac{d^2 \mathcal{G}}{dX^2} - A(1 - f_c) \Sigma_{\text{gas}}^\gamma = 0, \quad (2)$$

where the Kennicutt–Schmidt (KS) law $\dot{\Sigma}_* = A \Sigma_{\text{gas}}^\gamma$ is used for simplicity in the entire SF disk, A is a constant, and γ is the index (Kennicutt 1998)². Lynden-Bell & Pringle (1974) show

¹ Equation (1) is the modified version from Lin & Pringle (1987) and Wang et al. (2009b). We point out that $\dot{\Sigma}_{\text{SN}}$ is at $t - \tau_*$, where τ_* is the hydrogen main-sequence lifetime of stars depending on the stellar mass. Since stars form in the same gaseous disk, the stellar disk always follows the latter in the current model. Unless the stellar disk was formed in the previous episode, it could be larger than the gaseous disk, leading to reduce the feedback efficiency significantly (Nayakshin et al. 2007).

² We note that star formation rates may deviate from the KS law along the radii in the SF disk. It is not sufficiently understood (Krumholz et al. 2009), especially for so dense disks.

that $d\mathcal{G}/dX = \dot{M}$ at any radius, where \dot{M} is the mass rate of the inflows, provides the inner and outer boundary conditions. We employ the α -prescription viscosity as $\nu_{\text{SN}} = \alpha_{\text{SN}} V_{\text{tur}} H$, where α_{SN} is a constant, V_{tur} is the turbulence velocity driven by SNexp, and H is the thickness of the disk (Wada & Norman 2002; Wang et al. 2009b). The energy equation of the SNexp excited turbulence is given by

$$\frac{\rho_{\text{gas}} V_{\text{tur}}^2}{t_{\text{dis}}} = \frac{\rho_{\text{gas}} V_{\text{tur}}^3}{H} = \epsilon f_* \dot{\rho}_* E_{\text{SN}}, \quad (3)$$

where $t_{\text{dis}} = H/V_{\text{tur}}$ is the timescale of the turbulence, ϵ is the efficiency of converting kinetic energy of SNexp into turbulence, and $f_* \dot{\rho}_*$ is the density of SNexp rates. Here f_* is a number fraction of stars to the total mass of the formed stars, which are able to produce SNexp during one AGN episode. For a given IMF, we have $f_* = \int_{M_c}^{100M_\odot} N(M_*) dM_*/M_{\text{tot}}$ and $f_* \sim 2.3 \times 10^{-2} M_\odot^{-1}$ for $\beta = 2.35$. Considering $\dot{\Sigma}_* = \dot{\rho}_* H$ and $\Sigma_{\text{gas}} = \rho_{\text{gas}} H$, we have

$$\frac{V_{\text{tur}}^3}{H} = \epsilon f_* A E_{\text{SN}} \Sigma_{\text{gas}}^{\gamma-1}. \quad (4)$$

Following Paczynski (1978), we assume that gas rotates with a Keplerian velocity $\Omega_K = (GM_\bullet/R^3)^{1/2}$, where G is the gravity constant and M_\bullet is the SMBH mass. A vertical equilibrium holds among the disk self-gravity, SMBH gravity, and turbulent pressure. We usually have $dP_{\text{tur}}/dz = (\Omega^2 z + 2\pi G \Sigma_{\text{gas}}) \rho_{\text{gas}}$, where $P_{\text{tur}} = \rho_{\text{gas}} V_{\text{tur}}^2$ is the turbulence pressure and the second term is the self-gravity. Since the star formation supports the thickness of the SF disk, the self-gravity can be neglected (Thompson et al. 2005), allowing us to have an approximation form of vertical-averaged structure,

$$\frac{P_{\text{tur}}}{H} = \left(\frac{GM_\bullet}{R^3} H + 2\pi G \Sigma_{\text{gas}} \right) \rho_{\text{gas}} \approx \Omega_K^2 H \rho_{\text{gas}}. \quad (5)$$

We point out that the above equations are actually averaged in the vertical direction, and the parameters obtained in these equations are the values at the mid-plane of the SF disk.

The $\mathcal{G} - \Sigma_{\text{gas}}$ relation is specified for further simplification of Equation (2) through the viscosity ν . With the help of Equations (3)–(5), we have

$$\frac{d^2 \mathcal{G}}{dX^2} - \left(\frac{B}{X^2} \right)^2 \mathcal{G} = 0, \quad (6)$$

yielding an analytical solution in the form of

$$\mathcal{G}(X) = c_1 X \exp\left(\frac{B}{X}\right) + c_2 X \exp\left(-\frac{B}{X}\right), \quad (7)$$

where $B = 2GM_\bullet [(1 - f_c)/3\alpha_{\text{SN}} \epsilon f_* E_{\text{SN}}]^{1/2}$, $X = (GM_\bullet R)^{1/2}$ for the Keplerian rotation, and c_1 and c_2 are two constants determined by the boundary conditions. At the outer radius of the SF disk, only the mass injection rate is known and given by the mechanism of molecular cloud collisions (Krolik & Begelman 1988). We have $d\mathcal{G}/dX|_{X_{\text{out}}} = \dot{M}_{\text{out}}$, namely,

$$c_1 (1 - BX_{\text{out}}^{-1}) e^{\frac{B}{X_{\text{out}}}} + c_2 (1 + BX_{\text{out}}^{-1}) e^{-\frac{B}{X_{\text{out}}}} = \dot{M}_{\text{out}}, \quad (8)$$

where $X_{\text{out}} = (GM_\bullet R_{\text{out}})^{1/2}$. We assume that the inner radius of the SF disk is set to be the self-gravity radius (R_{sg}) of the

SS disk, which depends on the SMBH accretion rates (\dot{M}_\bullet). This yields $dG/dX|_{X_{\text{in}}} = \dot{M}_\bullet$, and subsequently

$$c_1 (1 - BX_{\text{sg}}^{-1}) e^{\frac{B}{X_{\text{sg}}}} + c_2 (1 + BX_{\text{sg}}^{-1}) e^{-\frac{B}{X_{\text{sg}}}} = \dot{M}_\bullet, \quad (9)$$

where $X_{\text{in}} = X_{\text{sg}} = (GM_\bullet R_{\text{sg}})^{1/2}$.

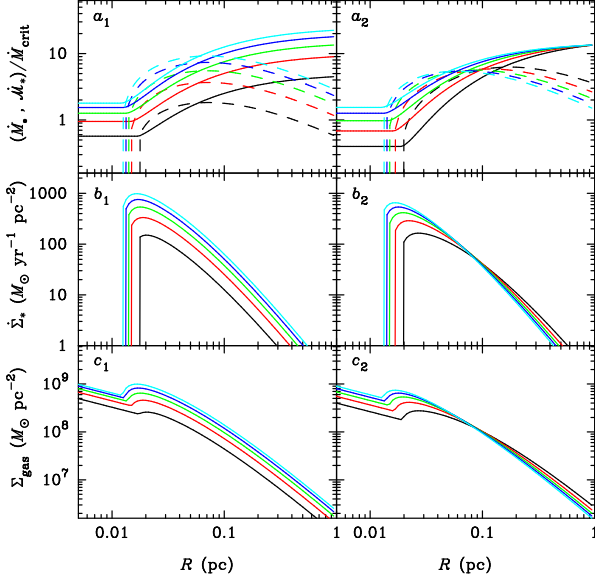


FIG. 2.— Structure of SF disks, which drive SS disks with an accretion rate of $0.5 - 2L_{\text{Edd}}/c^2$, as shown by the solid lines in a_1 . The panels on the left column are for $\epsilon = 0.5$, but \dot{M}_{out} takes 1.0, 2.0, 3.0, 4.0, $5.0M_\odot \text{yr}^{-1}$ represented by the black, red, green, blue, and cyan lines, respectively. The dashed lines are the local star formation rates defined by $\dot{\mathcal{M}}_* = \pi R^2 \dot{\Sigma}_*$, which are of $1 - 10M_\odot \text{yr}^{-1}$. The panels on the right column are the structures for fixed $\dot{M}_{\text{out}} = 3.0M_\odot \text{yr}^{-1}$, but $\epsilon = 0.2, 0.3, 0.4, 0.5, 0.6$ by black, red, green, blue, and cyan lines, respectively.

2.2. Switching on the Shakura–Sunyaev disk

The self-gravity instability develops when the Toomre’s parameter $Q \leq 1$. For the SS disk, the instability happens in the middle region of the SS disk at the radius

$$R_{\text{sg}} = 1068 \alpha_{0.1}^{14/27} M_8^{-26/27} \dot{m}^{-8/27} R_{\text{Sch}}, \quad (10)$$

where $R_{\text{Sch}} = 2GM_\bullet/c^2$ is the Schwarzschild radius, c is the light speed, $M_8 = M_\bullet/10^8 M_\odot$, $\dot{m} = \dot{M}_\bullet c^2/L_{\text{Edd}} = \dot{M}_\bullet/0.2M_8 M_\odot \text{yr}^{-1}$, L_{Edd} is the Eddington luminosity, and $\alpha_{0.1} = \alpha_{\text{SS}}/0.1$ is the viscosity parameter in the SS disk (see Kato et al. 1998). We assume that the SF process quenches within R_{sg} , and the SF disks smoothly switch on the SS disks at R_{sg} in term of surface density. The surface density of the SS disks is

$$\Sigma_{\text{SS}} = 8.2 \times 10^8 \alpha^{-4/5} M_8^{1/5} \dot{m}^{3/5} r_3^{-3/5} M_\odot \text{pc}^{-2}, \quad (11)$$

where $r_3 = R/10^3 R_{\text{Sch}}$, giving rise to the expression of the condition ($\Sigma_{\text{gas}} = \Sigma_{\text{SS}}$) of switching from the SF regions to the SS disk

$$c_1 e^{\frac{B}{X_{\text{sg}}}} + c_2 e^{-\frac{B}{X_{\text{sg}}}} = 3\pi\alpha\epsilon f_* A E_{\text{SN}} \Sigma_{\text{SS}}^\gamma \Omega^{-2}. \quad (12)$$

It is trivial to get the prolix expression of c_1 and c_2 from Equations (9) and (12), but we omit them here. We insert c_1 and c_2 into Equation (8) for the structure of the SF disk. Given R_{out} and \dot{M}_{out} , we can justify if the SF disk is able to drive the SS disk through solving equations (8), (9), (12). The accretion

rates of the SS disk as well as the structure of the SF disk are obtained self-consistently.

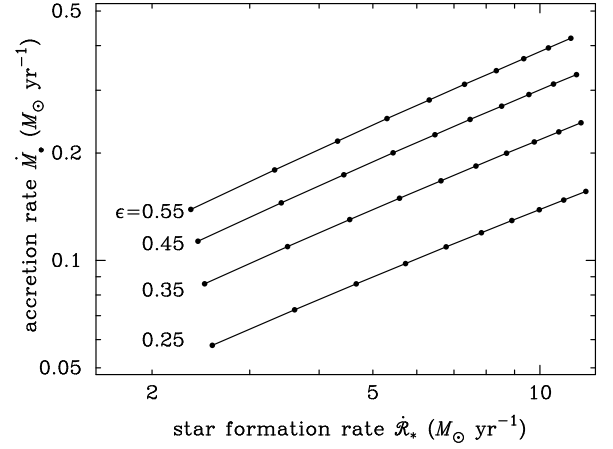


FIG. 3.— Relation between black hole accretion rates and the star formation rates in the SF disks. Each line represents a relation for the labeled ϵ . We find that a relation of $\dot{\mathcal{R}}_* \propto \dot{M}_\bullet^{1.4}$ and ϵ determines intercepts of the relation.

3. ACCRETION FLOWS APPROACHING TO SMBHS FROM SF DISKS

The empirical KS law $\dot{\Sigma}_* = A\Sigma_{\text{gas}}^\gamma$ is used, where $\gamma = 1.4$, $A = 2.5 \times 10^{-4}$, $\dot{\Sigma}_*$ and Σ_{gas} are in units of $M_\odot \text{yr}^{-1} \text{kpc}^{-2}$ and $M_\odot \text{pc}^{-2}$, respectively. We employ $E_{\text{SN}} = 10^{51} \text{erg}$, a top-heavy IMF index $\beta = 1.9$, $f_c = 0.63$, $f_* = 0.03M_\odot^{-1}$, $\alpha_{\text{SS}} = 0.2$, and $\alpha_{\text{SN}} = 1$ (in light of $D_{\text{SN}} \sim H$) throughout the paper. We take the outer radius $R_{\text{out}} = 1.0 \text{pc}$ and $M_\bullet = 10^8 M_\odot$, but adjust two parameters ϵ and \dot{M}_{out} to demonstrate the final accretion rates of SMBHs.

3.1. Structure of the SF disk

Figure $2a_1$ shows that the inflow driven by SNexp holds at a level of $\dot{M}_\bullet = 0.5 \sim 2\dot{M}_{\text{crit}}$ at the self-gravity radius ($R_{\text{sg}} \sim 0.02 \text{pc}$) for $\epsilon = 0.5$. This clearly demonstrates that an SF disk is able to drive an SS disk. Figure $2b_1$ plots $\dot{\Sigma}_*$ along the radial direction. We find that there is a peak of $\dot{\Sigma}_*$ in the SF disks before switching on an SS disk. This is caused by the star formation and the radial transportation of gas that compete along radii. From the second term of Equation (7), there is a cutoff of $\dot{\Sigma}_*$ and then an SF disk switches on an SS disk. Figure $2c_1$ displays a smooth transition of the surface density from SF disks to SS disks. The bumps in Figure $2c_1$ are artificially made by the assumption for simplicity that there is no star formation in the SS disk. This assumption roughly holds since the temperature within R_{sg} could be high enough to efficiently suppress star formation.

The right column of Figure 2 shows a dependence of the structure on ϵ for fixed \dot{M}_{out} . We find that \dot{M}_\bullet increases with ϵ , which appears in the exponential as shown in Equation (7). For $\dot{M}_{\text{out}} = 3M_\odot \text{yr}^{-1}$, the accretion rates are about 5%–10% \dot{M}_{out} from $\epsilon = 0.2 - 0.6$. The fraction $(1 - \epsilon)$ of the SNexp kinetic energy will be used to heat the gas of the SF disk, and then star formation is quenched close to the middle regions of SS disks. The output of this energy appears in the infrared bands in spectral energy distributions. Figure 3 shows the dependence of accretion rates on the global star formation rates, defined by $\dot{\mathcal{R}}_* = \int 2\pi \dot{\Sigma}_* R dR$. For a fixed ϵ , we find $\dot{\mathcal{R}}_* \propto \dot{M}_\bullet^q$, where $q = 1.43 - 1.56$ insensitive to \dot{M}_{out} .

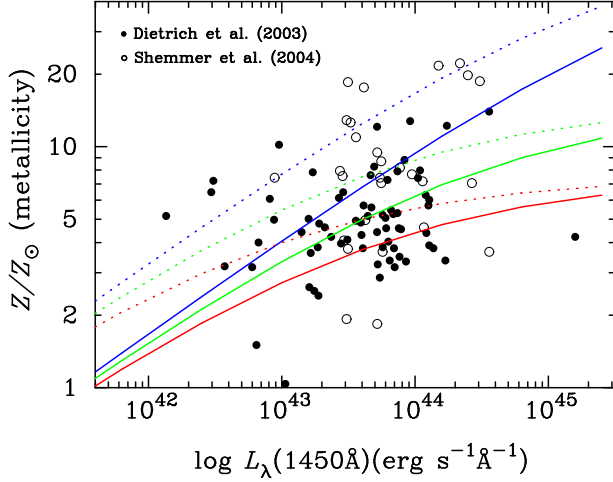


FIG. 4.— Comparison of the present model with the observed metallicity–luminosity relation. We use the theoretical relation $\log Z/Z_{\odot} = 1.0 + 1.33 \log(N \text{ v/C IV})$ (Hamann et al. 2002) to convert N v/C IV into Z for the Shemmer et al. (2004) sample. We employ the relation $L_{1450} \approx 2L_{5100} \approx (2/9)L_{\text{bol}}$, $L_{\text{bol}} \approx 9L_{5100} = \eta \dot{M}_{\bullet} c^2$ where η is the radiative efficiency and L_{bol} , L_{1450} , and L_{5100} are bolometric and specific luminosities at 1450Å and 5100Å, respectively. We use $Z_0 = 0$, $\varepsilon_1 = 20$, and $\varepsilon_2 = 0.1, 0.05, 0.01$ for red, green, and blue solid lines, respectively, whereas the dotted lines are for $\varepsilon_1 = 10$. The theoretical metallicity–luminosity relation is consistent with the observed.

It is necessary for AGNs and quasars to switch the SF disks from the middle region of the SS disks. We find that for lower \dot{M}_{out} the SF disks only support the outer region of the SS disk. In such a case, the SF disk may drive an advection-dominated accretion flow (ADAF) to SMBHs. Excellent examples of this case could be the Galactic center, some elliptical galaxies (e.g., M87), and LINERS, where star formation exhausts most of gas forming an ADAF as discussed by Tan & Blackman (2005). We would like to point out that β used here is only an intermediate top-heavy IMF. It has been suggested that $\beta = 0.85$ (Maness et al. 2007) and $\beta = 0.45$ (Bartko et al. 2010) in the Galactic center.

3.2. Relation Between metallicity and luminosity

Metals are ejected through SNexp enhancing the metallicity in the SF disk. The mass of the metal element $-i$ produced by SNexp is given by $M_{Z_i} = \int_{M_1}^{M_2} dM_* N(M_*) \dot{\mathcal{R}}_* m_i^{\text{ej}}(M_*, Z_*)$, where $m_i^{\text{ej}}(M_*, Z_*)$ is the ejected mass of the element $-i$ dependent on the initial mass and metallicity of progenitor stars (Woosley & Weaver 1995; Gavilan et al. et al. 2005). With the M_{Z_i} , the total ejected metal is then calculated by $M_Z = \sum_i M_{Z_i}$. For simplicity, we take an approximation of the metal fraction $m_Z = M_Z/M_* \approx 0.1 - 0.2$ (Woosley & Weaver 1986).

Detailed calculations of metallicity involve evolution of stellar populations in the SF disk, advection of metal-enriched gas, and star formation, which make a strong radial dependence of metallicity complicated. However, we study the mean metallicity Z , as the observed, in the SF disk by introducing ε_1 and ε_2 . Considering the radial dependence of metallicity, $\varepsilon_1 Z$ will be swallowed by SMBHs while $\varepsilon_2 Z$ is consumed by star formation. The lower limit of metallicity at radius R is roughly given by $Z \approx f_c m_Z \dot{\mathcal{M}}_*/\dot{M}_{\bullet}$, and we have $\varepsilon_1 \geq Z_{\text{in}}/Z \sim \dot{\mathcal{M}}_*/\dot{M}_{\bullet} \sim 5$ from Figure 2(a_1), where the (sub/super) script “in” means the val-

ues of parameters at the inner edge of the SF disk, and $\dot{\mathcal{M}}_*$ is the local SF rates. On the other hand, its upper limit is $Z_{\text{max}}/Z \sim f_c m_Z \dot{\mathcal{R}}_*/\dot{M}_{\bullet} Z \sim 30/(Z/Z_{\odot})$, where we use $f_c = 0.6$ and $m_Z = 0.1$. So we have $5 \leq \varepsilon_1 \leq 30$ if the mean $Z \sim Z_{\odot}$. The parameter $\varepsilon_2 \sim Z_0/Z \sim 0.1$ for $Z_0 = 0.1 Z_{\odot}$.

The total mass of the metal by time t through integrating the net increase of metals is given by $M_Z(t) = \int_0^t (Z_0 \dot{M}_{\text{out}} + f_c \dot{\mathcal{R}}_* m_Z - \varepsilon_1 Z \dot{M}_{\bullet} - \varepsilon_2 Z \dot{\mathcal{R}}_*) d\tau$, where Z_0 is the initial metallicity of the gas supplied from the torus. The first term in the integration is contributed by the initial metal of supplied gas, the second is contributed by SNexp, the third is advected into SMBH and the last one is the consumption of metals during star formation. The total gas of the SF disk is given by $M_{\text{gas}}(t) = \int_0^{R_{\text{out}}} 2\pi \Sigma_{\text{gas}}(t, R) R dR$. We obtain the metallicity at time t by its definition of $Z(t) = M_Z(t)/M_{\text{gas}}(t)$

$$Z(t)M_{\text{gas}}(t) = \int_0^t (Z_0 \dot{M}_{\text{out}} + f_c \dot{\mathcal{R}}_* m_Z - \varepsilon_1 Z \dot{M}_{\bullet} - \varepsilon_2 Z \dot{\mathcal{R}}_*) d\tau. \quad (13)$$

This is an integral-differential equation, which is easy to understand in light of Z as an integral parameter with time. For a steady SF disk, its total mass is a constant, but metals are increasing. After some algebraic manipulations, we have its solution

$$Z(t) = Z_{\text{max}} + (Z_0 - Z_{\text{max}}) \exp\left(-\frac{t}{t_Z}\right), \quad (14)$$

where $Z_{\text{max}} = (Z_0 \dot{M}_{\text{out}} + f_c \dot{\mathcal{R}}_* m_Z)/(\varepsilon_1 \dot{M}_{\bullet} + \varepsilon_2 \dot{\mathcal{R}}_*)$, $t_Z = M_{\text{gas}}/(\varepsilon_1 \dot{M}_{\bullet} + \varepsilon_2 \dot{\mathcal{R}}_*)$, and $Z(0) = Z_0$ is assumed initially. For a time long enough, the last term will tend to zero, we have

$$Z_{\text{max}} = Z_0(1 - \Lambda) + f_c(m_Z - Z_0)\Lambda \approx \frac{c_0 f_c m_Z}{\varepsilon_1 + \varepsilon_2 c_0} \dot{M}_{\bullet}^{0.4}, \quad (15)$$

where $\Lambda = \dot{\mathcal{R}}_*/(\varepsilon_1 \dot{M}_{\bullet} + \varepsilon_2 \dot{\mathcal{R}}_*)$, $\dot{M}_{\text{out}} = (1 - f_c) \dot{\mathcal{R}}_* + \dot{M}_{\bullet}$ is used, \dot{M}_{\bullet} is in units of $M_{\odot} \text{ yr}^{-1}$, $\dot{\mathcal{R}}_* = c_0 \dot{M}_{\bullet}^{1.4}$, and $c_0 = 43.03$ insensitive to M_{\bullet} for $\epsilon = 0.5$. The approximation is valid only for $Z_0 \ll m_Z$. We assume for a comparison with observational data that most of quasars reach the state with maximum metallicity, but the episodic age of quasars can be estimated from Equation (14) if the metallicity is measured accurately enough.

Figure 4 shows a comparison of the model with data. Not only the metal-rich phenomenon in quasars is explained, but also the Z - L relation is reproduced by the present model. The large scatters of the Z - L relation imply different ε_1 , ε_2 , and c_0 individually.

3.3. Compact nuclear star clusters

The present model may predict the formation of nuclear star clusters commonly found in local galaxies. They are 1-2 orders of magnitude brighter than globular clusters (Côté et al. 2006), have extended star formation histories (Rossa et al. 2006), complex morphologies (Seth et al. 2006), and follow the relation similar to the Magorrian relation (Ferrarese et al. 2006). Though the SF disk discussed here is only on a scale of 1 pc, SF is ongoing inside the torus at a few 10 pc scale (Collin & Zahn 1999), which is invisible due to dust extinction. Since AGN types are irrelevant to orientations of their host galaxies (e.g., Munoz Marin et al. 2007), SMBHs are randomly fed by the dusty torus. This is evidence for random accretion onto the SMBHs, which is derived from the

η -equation (Wang et al. 2009a) and is confirmed by calculations based on the semi-analytical theory of mergers (Li et al. 2010). One stellar belt with random direction composed of old stars is left after one episodic activity accordingly. The appearance of the nuclear star cluster could be a natural consequence of the multiple episodes of SMBH activities (Wang et al. 2008; Wang et al. 2009a). The clusters are thus tightly related to the central SMBHs in the present model. Figure 3 suggests that a mass ratio of SMBH and a nuclear star cluster is roughly 0.01-0.1 depending on ϵ and β (i.e., star formation history), consistent with the observations (Seth et al. 2008). Detailed comparison with observed properties of the clusters, such as radial-dependent metallicity, SF history, will provide further clue to understand physics in galactic centers.

All the emission from the SF disk will be thermalized with a typical temperature of $T_{\text{SF}} \sim (L_{\text{SN}}/2\pi R_{\text{SF}}^2 \sigma_{\text{SB}})^{1/4} \sim 2000 L_{\text{SN},43}^{1/4} \text{K}$ in the near-infrared band, where σ_{SB} is the Stefan-Boltzman constant, $L_{\text{SN},43} = L_{\text{SN}}/10^{43} \text{erg s}^{-1}$ is the SNexp luminosity. It then contributes a fraction to the observed infrared emissions in quasars, which is worth investigating further.

4. CONCLUSIONS AND DISCUSSIONS

We show that an SF disk supplied by the dusty torus is able to support an SS disk around SMBHs in AGNs and quasars. Such a model naturally produces the observed relationship between metallicity and luminosity. As a natural consequence of the multiple episodes of activity through random accretion onto the holes, a nuclear star cluster will be formed from the remnants of stellar disks. The present model would provide a unified explanation of feeding SMBHs, production of metallicity, and formation of a nuclear star cluster.

We stress that the present paper deals with the stationary structure of SF disks switching to SS disks. A time-dependent model will give the evolution of AGNs driven by the SF disks for the complicated AGN–starburst connection.

The anonymous referee is thanked for a helpful report. H. Netzer is acknowledged for interesting discussions. We appreciate the stimulating discussions among the members of the IHEP AGN group. The research is supported by NSFC-10733010 and 10821061, CAS-KJCX2-YW-T03, and 973 project (2009CB824800).

REFERENCES

- Bartko, H. et al. 2010, *ApJ*, 708, 834
 Barvainis, R. 1987, *ApJ*, 320, 537
 Bonnell, I. A. & Rice, W. K. M. 2008, *Science*, 321, 1060
 Brunner, H. et al. 1997, *A&A*, 326, 885
 Chen, Y.-M., et al. 2009, *ApJ*, 695, L130
 Collin, S. & Zahn, J.-P. 1999, *A&A*, 344, 433
 Côté, P. et al. 2006, *ApJS*, 165, 57
 Dietrich, M. et al. 2003, *ApJ*, 589, 722
 Ferrarese, L. et al. 2006, *ApJ*, 644, L42
 Goodman, J. 2003, *MNRAS*, 339, 937
 Hamann, F. & Ferland, G. 1999, *ARA&A*, 37, 487
 Hamann, F. et al. 2002, *ApJ*, 564, 592
 Hobbs, A. & Nayakshin, S. 2009, *MNRAS*, 394, 191
 Hobbs, A. et al. 2010, *MNRAS*, arXiv:1001.3883
 Hu, C., et al. 2008, *ApJ*, 687, 78
 Hu, C., et al. 2008, *ApJ*, 683, L115
 Kato, S., Fukue, J. & Mineshige, S. 1998, in *Black-Hole Accretion Disks*, ed. S. Kato, J. Fukue, & S. Mineshige (Kyoto, Japan: Kyoto Univ. Press), chap. 3
 Kennicutt, R. C. 1998, *ARA&A*, 36, 189
 Kolykhalov, P. I. & Sunyaev, R. A. 1980, *Sov. Astron. Lett.*, 6, 357
 Krolik, J. & Begelman, M. C. 1988, *ApJ*, 329, 702
 Krumholz, M. R., McKee, C. F. & Tumlinson, J. 2009, *ApJ*, 693, 216
 Kormendy, J., et al. 2009, *ApJS*, 182, 216
 Kumar, P. & Johnson, J. L. 2010, *MNRAS*, 404, 2170
 Laor, A. & Netzer, H. 1989, *MNRAS*, 238, 897
 Li, Y.-R., et al. 2010, *ApJ*, 710, 878
 Lin, D. N. C. & Pringle, J. E. 1987, *ApJ*, 320, L87
 Lü, X.-R. 2008, *Chin. J. Astron. Astrophys.*, 8, 50
 Lynden-Bell, D. & Pringle, J. 1974, *MNRAS*, 168, 603
 Maness, H. et al. 2007, *ApJ*, 669, 1024
 Mor, R., Netzer, H. & Elitzur, M. 2009, *ApJ*, 705, 298
 Munoz-Marin, V. M. et al. 2007, *AJ*, 134, 648
 Nayakshin, R. & Sunyaev, R. 2005, *MNRAS*, 364, L23
 Nayakshin, R., Cuadra, J., & Springel, V. 2007, *MNRAS*, 379, 21
 Paczynski, B. 1978, *Acta Astron.*, 28, 91
 Paumard, T. et al. 2006, *ApJ*, 643, 1011
 Rossa, J. et al. 2006, *AJ*, 132, 1074
 Seth, A. et al. 2006, *AJ*, 132, 2539
 Seth, A. et al. 2008, *ApJ*, 678, 116
 Shemmer, O. et al. 2004, *ApJ*, 614, 547
 Shlosman, I. & Begelman, M. C. 1987, *Nature*, 329, 810
 Sun, W.-H. & Malkan, M. A. 1989, *ApJ*, 346, 68
 Tan, J. C. & Blackman, E. G. 2005, *MNRAS*, 362, 983
 Thompson, T., Quataert, E. & Murray, N. 2005, *ApJ*, 630, 167
 Wada, K. & Norman, 2002, *ApJ*, 566, L21
 Wang, J.-M., Chen, Y.-M., Yan, C.-S. & Hu, C., 2008, *ApJ*, 673, L9
 Wang, J.-M., Chen, Y.-M. & Zhang, F. 2006, *ApJ*, 647, L17
 Wang, J.-M., et al. 2009a, *ApJ*, 697, L141
 Wang, J.-M., et al. 2009b, *ApJ*, 701, L7
 Woosley, S. E. & Weaver, T. A. 1986, *ARA&A*, 24, 205
 Yu, Q. & Tremaine, S. 2002, *MNRAS*, 335, 965